Assessment on Image Quality Changes as a Result of Implementing Median Filtering, Wiener Filtering, Histogram Equalization, and Hybrid Methods on Noisy Images

R. Rizal Isnanto
Department of Computer Engineering
Diponegoro University
Semarang, Indonesia
email: rizal@ce.undip.ac.id

Yudi Eko Windarto
Department of Computer Engineering
Diponegoro University
Semarang, Indonesia
email: email: yudi@live.undip.ac.id

Mutiara Victorina Mangkuratmaja
Department of Computer Engineering
Diponegoro University
Semarang, Indonesia
mutiaravm@student.ce.undip.ac.id

***Abstract*— The information content in an image can experience a decrease in quality due to noises. Accordingly, noise removal and histogram equalization (HE) are among the processes used to enhance image quality. The purpose of this research is to determine the effect of changes in image quality as a result of applying median filtering (MF), Wiener filtering (WF), HE, or hybrid methods on noisy images. Here, face images are used as input. The research stages began with preprocessing, i.e., cropping, size normalization, and color-to-gray conversion. Then, Gaussian and salt-and-pepper noises with intensities of 20%, 50%, and 80% are applied to the images. Consequently, the processes, i.e., HE, MF, WF, hybrid method 1 (HE and MF), and hybrid method 2 (HE and WF), are implemented, and then the image quality is evaluated. The results of the research show that the best methods to enhance Gaussian and salt-and-pepper noisy images are WF and MF, respectively. HE and the two hybrid methods generally do not improve image quality. The implementation of hybrid method 2 results in the maximum structural similarity index with 80% Gaussian noise. Meanwhile, MF provides the minimum mean-square error and maximum peak signal-to-noise ratio with 20% Gaussian noise.**

Keywords — histogram equalization, median filtering, Wiener filtering, Gaussian noise, salt-and-pepper noise

I. Introduction

Image data acquisition sometimes results in poor quality images. The information content in an image can experience a decrease in quality due to noises. Accordingly, noise removal and histogram equalization (HE) are among the examples of processes to enhance image quality. Image enhancement methods are required to improve the quality of images and maximize the information content that exists in the input image so that it can obtain a form of visualization that is better and more easily interpreted by humans and computer machines. The most commonly used image enhancement methods are HE, Wiener filtering (WF), and median filtering (MF) [1].

The purpose of this research is to determine the effect of changes in image quality as a result of applying MF, WF, HE, and hybrid methods on noisy images. The hybrid methods proposed in this research are hybrid method 1 (HE + MF) and hybrid method 2 (HE + WF).

II. Previous Works

Erwin *et al.* examined three image enhancement methods, i.e., image sharpening, contrast enhancement, and standard MF. The image quality parameters used in this study are based on mean-square error (MSE), peak signal-to-noise ratio (PSNR), and structural similarity index (SSIM) values. The results of this study indicate that the highest PSNR, MSE, and SSIM values were obtained in the implementation of the MF method with PSNR = 37.83, MSE = 145.81, and SSIM = 0.97 [2]. George *et al.* concluded that median-based filters are commonly used to remove impulse noises. Some types of MF include recursive MF, iterative MF, directional MF, weighted MF, adaptive MF, progressive switching median (PSM) filter, and threshold MF [3].

Kunsoth and Binwas proposed a modified decision-based MF for impulse noise removal. Their experimental results show that the proposed method performs better than the standard MF, weighted MF, adaptive MF, and decision-based MF, especially when a high noise intensity level [4]. Priestley *et al.* proposed a decision-based switching MF for image restoration. The performance of this algorithm was tested against four noise models with different levels of noise densities and was evaluated in terms of performance metrics, including PSNR and IEF. It provided better results for images that were extremely corrupted with up to 90% noise density and outperformed classic filters in terms of handling image corruption [5].

Darus *et al.* proposed a modified hybrid MF for the removal of low-density random-valued impulse noise in images. This technique has been proven to be capable of overcoming the shortcomings of a standard MF and improve the hybrid MF in restoring image details and operating at high noise densities [6]. Khatri and Kasturiwale conducted a computer analysis to analyze the performance of the proposed method with that of simple MF, simple adaptive MF, and adaptive switched MF. The proposed filter was proven to be more efficient in terms of objective and subjective parameters [7]. Goyal and Chaurasia explained that random-valued impulse noise is the most frequent cause of distortion in natural images [8].

Lahmiri and Boukadoum proposed a combination of WF and partial differential equation (PDE) filtering to form a sequential hybrid filter. Their experimental results showed the superiority of the proposed system over using either the

local WF or PDE filter alone [9]. Baselice *et al*. proposed an enhanced WF for despeckling ultrasound images. This technique can locally adapt the noise filtering intensity to combine good edges and detail preservation with effective noise reduction [10]. Arazm *et al*. proposed the noise reduction of scanning electron microscope (SEM) images using adaptive WF. The proposed filter was compared with the original WF, i.e. before modified to be adaptive WF, to denoise SEM images. For different noise variances, the experimental results indicate that the proposed filter has better performance compared with other filters [11]. Sheer and Al-Ani investigated the effects of a regularization parameter (α), via non-blind iterative WF, for restoring a medical image. The best result which measured by SNR parameter was obtained with $\alpha = 1$ and with a small width of the blurring function and high values of SNR [12].

Kalavathi and Priya studied the removal of impulse noise using histogram-based localized WF for MR brain image restoration. The performance of this method was evaluated by calculating the PSNR value. Their experimental results show that the proposed method gives better results on denoising impulse noises in medical images compared with existing methods, i.e., anisotropic diffusion filter, bilateral filter, non-local mean filter, and WF [13]. The review on HE-based image enhancement techniques by Nithyanand *et al*. indicated that noise removal, contrast improvement, and adjustment of brightness are common operations performed on raw images captured by a camera. They also concluded that HE is an important image enhancement scheme and proposed many variations of HE [14].

III. Research Method

The research stages are shown in Fig. 1.

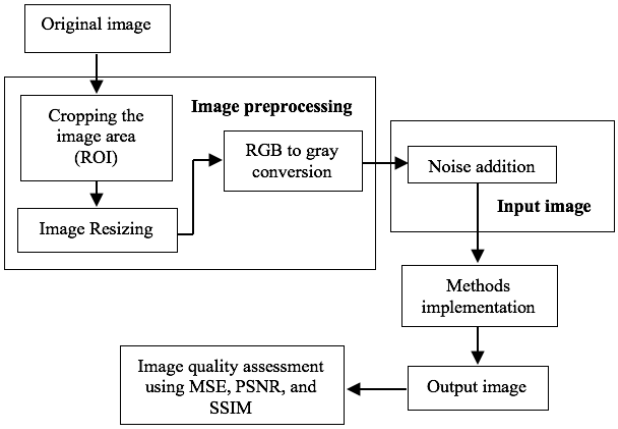

Fig. 1. Research stages

A. Image Preprocessing

The purpose of preprocessing is to focus certain parts of the input image (determining the region of interest [ROI]), with a uniform type, i.e., gray image, and size. We used facial images of various expressions as the input images. The first step is image cropping, where the images containing the face were cropped so that only the face part is captured.

Then, the images were resized to 224 x 224 pixels to normalize the image size. After that, the images were converted from RGB to grayscale. The resulting images after the three processes were used as the reference images that were compared with the output images after the noise addition and image enhancement. Examples of the images after cropping the facial area, resizing, and converting from RGB to grayscale are shown in Fig. 2.

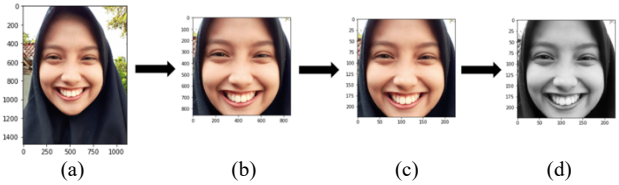

Fig. 2. Example of the process stages: (a) original image; (b) cropping the facial area; (c) image resizing; (d) RGB to grayscale conversion.

B. Input Image

The input images were the preprocessing results before and after the addition of noises. The noises added were Gaussian noise and salt-and-pepper noise with intensities of 20%, 50%, and 80%. The resulting images were used as the input images for the image enhancement method. Figure 3 shows examples of images before and after the addition of Gaussian noises with intensities of 20%, 50%, and 80%.

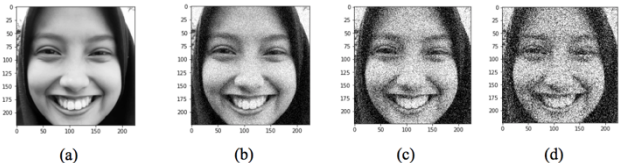

Fig. 3. Example of Gaussian noise addition effects: (a) original image; (b) 20% intensity; (c) 50% intensity; (d) 80% intensity.

Figure 4 shows examples of images before and after the addition of salt-and-pepper noise with intensities of 20%, 50%, and 80%.

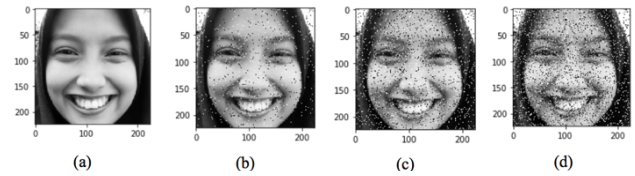

Fig. 4. Example of salt-and-pepper noise addition effects: (a) original image; (b) 20% intensity; (c) 50% intensity; (d) 80% intensity.

C. Method Implementation

In this research, five variations of the method are implemented: (1) HE, (2) MF, (3) WF, (4) hybrid 1 (HE + MF), and (5) hybrid 2 (HE + WF). HE increases the dynamic range of gray levels in a low-contrast image to cover the full range of gray levels [15]. In HE, the new pixel value x is calculated by

$$I(x) = \text{round}\left[\frac{\text{CDF}(x)-\min \text{CDF}}{1-\min \text{CDF}}\right] \times (L-1). \quad (1)$$

The cumulative distribution function (CDF) of an image is calculated using the following formula:

$$\text{CDF}[k] = \sum_{j=0}^{k} 255 \; {}^{n_j}/_{N}, \quad (2)$$

where CDF[k] is the CDF value of a pixel with value k in the input image, n_j is the number of pixels with value j, and N is the total number of pixels. All input pixels with corresponding values CDF[k] have to re-labeled [16].

When implementing the MF, a 3 x 3 filtering window was used. The median was derived from the nine neighboring pixels using Eq. 3 [17].

$$M(i,j) = \text{median}\,[X(i\text{-}1\,,j\text{-}1), X(i\text{-}1\,,j), \ldots X(i\text{-}1\,,j\text{+}1), X(i\,,j\text{-}1), X(i\,,j), X(i\,,j\text{+}1)\ldots X(i\text{+}1\,,j\text{-}1), X(i\text{+}1\,,j), X(i\text{+}1\,,j\text{+}1)], \quad (3)$$

where $M(i,j)$ is the median value that will replace the pixel value at the position (i,j) and $X(m,n)$ is the pixel value at the position (m,n).

The WF was implemented in this research to estimate the local mean and variance around each pixel:

$$\mu = \frac{1}{NM}\sum_{n_1,n_2\in\eta} a(n_1,n_2) \quad (4)$$

$$\sigma^2 = \frac{1}{NM}\sum_{n_1,n_2\in\eta} a^2(n_1,n_2) - \mu^2, \quad (5)$$

where $\eta$is the N-by-M local neighborhood of each pixel in image A. The software then created a pixel-wise WF using the following estimates:

$$b(n_1,n_2) = \mu + \frac{\sigma^2-v^2}{\sigma^2}(a(n_1,n_2)-\mu), \quad (6)$$

where v^2 is the noise variance. If no noise variance is given, then the software implementation uses the average of all the local estimated variances [18].

D. Image Quality Assessment

The assessment was conducted quantitatively with the MSE, PSNR, and SSIM parameters. The values of the three parameters were used as the determinants of the optimal method that provided the best output image.

The MSE was used to obtain the sum of the squares of the "errors" between the original image $s(i,j)$ and filtered output image $y(i,j)$. The pixels $s(i,j)$ correspond to $1 \le i \le M_1$ and $1 \le j \le M_2$ [19].

$$MSE = \frac{\sum_i^{M_1}\sum_j^{M_2}[y(i,j)-s(i,j)]^2}{M_1 \times M_2}. \quad (7)$$

The PSNR was used to estimate the robustness of denoising with respect to the noise. The PSNR between the original image $s(i,j)$ and filtered output image $y(i,j)$ of dimension $M_1 \times M_2$ is defined as [20]

$$PSNR = 10 \times \log_{10}\frac{P^2}{MSE}, \quad (8)$$

where P = maximum value in the original image.

The SSIM estimates the similarity measure between the original image $s(i,j)$ and filtered output image $y(i,j)$. SSIM is defined as [20]

$$SSIM = \frac{(2\,\mu_s\mu_y + c_1)(2\,\sigma_{sy} + c_2)}{(\mu_s^2 + \mu_y^2 + c_1)(\sigma_s^2 + \sigma_y^2 + c_2)}, \quad (9)$$

where μ_s is the local mean of the original image s, μ_y is the local mean of output image y, and σ_{sy} is the standard deviation between s and y. σ_s^2 denotes the variance of s. $c_1 = (K_1L)^2$, $c_2 = (K_2L)^2$, $K_1 = 0.01$, and $K_2 = 0.03$ by default, and L is the dynamic range of pixel values [20].

IV. Results and Discussion

In this research, Gaussian and salt-and-pepper noises with intensity variations of 20% (low-level noise), 50% (medium-level noise), and 80% (high-level noise) were added. To determine the optimal method for image enhancement, the image quality was measured in terms of the MSE, PSNR, and SSIM values. Figure 5 shows the five input images used as references to the output images.

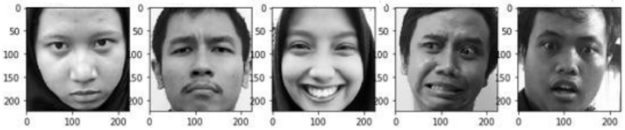

Fig. 5. Five preprocessed face images in various expressions:(a) angry; (b) sad; (c) happy; (d) scared; and (e) shocked.

We used five input images with different facial expressions, i.e., sad, angry, happy, shocked, and scared. Two different noises were added to the five images: Gaussian noise and salt-and-pepper noise. The noise intensity was determined by three types of levels: 20% (low-level noise intensity), 50% (medium-level noise intensity), and 80% (high-level noise intensity). Then, an image enhancement process was conducted using six schemes (no enhancement, HE, MF, WF, hybrid 1, and hybrid 2). Three measurement parameters, i.e., MSE, PSNR, and SSIM, were used to assess the image quality of the original images before the noises were added. From the description above, there are 5 x 2 x 3 x 6 x 3 = 540 tests. To summarize the research results, the testing results of the five different facial expressions for one testing scheme were averaged. Table I shows the test results of the Gaussian noise-added images in the no-enhancement process. Table II shows the test results of the salt-and-pepper noise-added images in the no-enhancement process (note: in both tables, label 1 = angry; 2 = sad; 3 = happy; 4 = scared; 5 = shocked).

TABLE I. Test Results for the Gaussian Noise-added Images for the No-enhancement Process

Intensity	Para-meters	Facial expression images					Average
		1	2	3	4	5	
20%	MSE	373.2	390.8	362.3	386.7	381.9	379.0
	PSNR	22.41	22.21	22.54	22.26	22.31	22.35
	SSIM	0.32	0.32	0.36	0.32	0.32	0.33
50%	MSE	2025	2151	1984	2091	2147	2079.9
	PSNR	15.07	14.80	15.15	14.93	14.81	14.92
	SSIM	0.107	0.11	0.135	0.104	0.103	0.112
80%	MSE	4424	4593	4214	4457	4575	4452.9
	PSNR	11.67	11.5	11.88	11.64	11.53	11.64
	SSIM	0.055	0.058	0.075	0.053	0.054	0.059

TABLE II. Test Results for the Salt-and-pepper Noise-added Images for the No-enhancement Process

Intensity	Para-meters	Facial expression images					Average
		1	2	3	4	5	
20%	MSE	863	731	889	844	770	819.6
	PSNR	18.8	19.5	18.6	18.9	19.3	19.0
	SSIM	0.78	0.79	0.80	0.78	0.79	0.79
50%	MSE	2148	1931	2170	2086	2037	2074.2
	PSNR	14.8	15.3	14.8	14.9	15.0	14.9
	SSIM	0.54	0.54	0.57	0.53	0.54	0.54
80%	MSE	3382	3059	3465	3360	3202	3293.7
	PSNR	12.8	13.3	12.7	12.9	13.1	13.0
	SSIM	0.37	0.36	0.40	0.36	0.37	0.37

The test was performed on the five image enhancement processes, i.e., HE, MF, WF, hybrid 1, and hybrid 2. As shown in Tables 1 and 2, the parameter values of the MSE, PSNR, and SSIM on the same noise type and noise intensity produce almost similar values. For the other five tests, the same condition applies. Therefore, the succeeding research results are given in the form of an average value, not the individual value of the image type test. Tables III and IV respectively show the average values of the whole test with the addition of Gaussian and salt-and-pepper noises.

TABLE III. AVERAGE TEST RESULT VALUES FOR THE GAUSSIAN NOISE-ADDED IMAGES

Methods	Noise intensity	MSE	PNSR	SSIM
No enhancement	20%	379.00	22.35	0.33
	50%	2079.85	14.95	0.11
	80%	4452.85	11.64	0.06
Averaged		**2303.90**	**16.31**	**0.17**
Histogram equalization (HE)	20%	886.59	18.85	0.28
	50%	2498.27	14.17	0.11
	80%	4543.84	11.56	0.06
Averaged		**2642.90**	**14.86**	**0.15**
Median filtering (MF)	20%	189.54	25.69	0.66
	50%	535.49	20.89	0.35
	80%	1113.36	17.67	0.21
Averaged		**612.80**	**21.42**	**0.41**
Wiener filtering (WF)	20%	270.17	23.82	0.65
	50%	485.06	21.27	0.38
	80%	868.25	18.75	0.25
Averaged		**541.16**	**21.28**	**0.43**
Hybrid 1 (HE + MF)	20%	547.77	21.10	0.58
	50%	751.54	19.44	0.33
	80%	1286.39	17.06	0.21
Averaged		**861.90**	**19.20**	**0.37**
Hybrid 2 (HE + WF)	20%	546.17	21.01	0.60
	50%	588.56	20.47	0.37
	80%	978.04	18.25	0.25
Averaged		**704.26**	**19.91**	**0.41**

TABLE IV. AVERAGE TEST RESULT VALUES FOR THE SALT-AND-PEPPER NOISE-ADDED IMAGES

Methods	Noise intensity	MSE	PNSR	SSIM
No enhancement (NE)	20%	819.556	19.006	0.787
	50%	2074.294	14.965	0.541
	80%	3293.689	12.958	0.373
Averaged		**2062.51**	**15.64**	**0.57**
Histogram equalization (HE)	20%	1200.74	17.373	0.715
	50%	2375.25	14.372	0.496
	80%	3561.21	12.616	0.34
Averaged		**2379.07**	**14.79**	**0.52**
Median filtering (MF)	20%	119.066	28.886	0.94
	50%	132.68	27.92	0.93
	80%	160.9	26.629	0.916
Averaged		**137.55**	**27.81**	**0.93**
Wiener filtering (WF)	20%	376	22.393	0.623
	50%	538.006	20.83	0.428
	80%	739.191	19.452	0.324
Averaged		**551.07**	**20.89**	**0.46**
Hybrid 1 (HE + MF)	20%	509.336	21.514	0.861
	50%	462.8	21.771	0.853
	80%	476.703	21.57	0.839
Averaged		**482.95**	**21.62**	**0.85**
Hybrid 2 (HE + WF)	20%	667.684	20.067	0.602
	50%	768.095	19.342	0.423
	80%	926.91	18.503	0.323
Averaged		**787.56**	**19.30**	**0.45**

The observation values are summarized as the average values of the overall implementation of six variations, consisting of one variation without the enhancement method and five variations of the image enhancement implementation. The six variations can be shown in Table V.

TABLE V. AVERAGE VALUES OF THE MSE, PSNR, AND SSIM FOR THE GAUSSIAN AND SALT-AND-PEPPER NOISE-ADDED IMAGES

Methods	Parameters	Gaussian noise	Salt-and-pepper noise
No enhancement	MSE	2303.90	2062.51
	PSNR	16.31	15.64
	SSIM	0.17	0.57
Histogram equalization (HE)	MSE	2642.9	2379.07
	PSNR	14.861	14.787
	SSIM	0.15	0.517
Median filtering (MF)	MSE	612.796	**137.549**
	PSNR	**21.415**	**27.812**
	SSIM	0.406	**0.929**
Wiener filtering (WF)	MSE	**541.162**	551.066
	PSNR	21.28	20.892
	SSIM	**0.428**	0.458
Hybrid 1 (HE + MF)	MSE	861.898	482.946
	PSNR	19.2	21.618
	SSIM	0.372	0.851
Hybrid 2 (HE + WF)	MSE	704.255	787.563
	PSNR	19.912	19.304
	SSIM	0.407	0.449

For the MSE parameters, the optimal method produced the minimum MSE value. For the PSNR and SSIM parameters, the optimal method produced the maximum PSNR and SSIM values. The optimal values are indicated by bold letters in Table V.

A. Gaussian Noise Addition

Table 5 shows that the addition of Gaussian noise will be optimally enhanced by WF because the minimum MSE and maximum SSIM values are obtained in the implementation of WF.

The maximum average PSNR value was determined with the application of MF. However, two of the three individual values from the PSNR test show the maximum value in the implementation of WF, as shown in Table 3. The two maximum PSNR values are for additional noise with noise intensities of 50% and 80% and PSNR of 21.27 and 18.75. In the application of MF, the maximum value was obtained with the Gaussian noise addition with an intensity of 20% (PSNR = 25.69). This extreme value resulted in an average PSNR being higher than that in the MF. Thus, Gaussian noise can be more enhanced using WF rather than MF. This conclusion is in accordance with that conveyed by George *et al.* [3], Vishaga and Das [21], and Sravani *et al.* [22]. Figure 6 explains the advantages of WF in enhancing Gaussian noisy images.

Exception testing of hybrid method 2 (HE and WF) provided a maximum SSIM on high-Gaussian-noise images (80%). Meanwhile, the MF was better because it provided the minimum MSE and maximum PSNR for the low-Gaussian-noise images (20%). However, these exclusions do not affect the conclusion that, on average, for overall testing, WF can best enhance the quality of Gaussian noise images rather than the other methods.

B. Salt-and-pepper Noise Addition

Figure 7 depicts the graph of the three parameters, i.e., MSE, PSNR, and SSIM, to assess the image enhancement methods with the salt-and-pepper noise addition. This figure also indicates the advantages of MF in enhancing the salt-

and-pepper noisy images. Table V and Fig. 7 show that the addition of salt-and-pepper noise will be optimally enhanced by implementing MF because the minimum MSE, maximum PSNR, and maximum SSIM values are obtained in applying the process. This conclusion coincides with that of Mehta [17], Lahmiri and Boukadoum [9], Arazm *et al.* [11], and Sheer and Al-Ani [12].

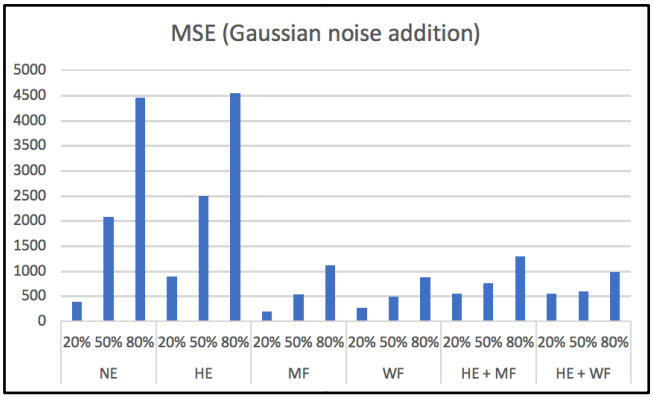

(a)

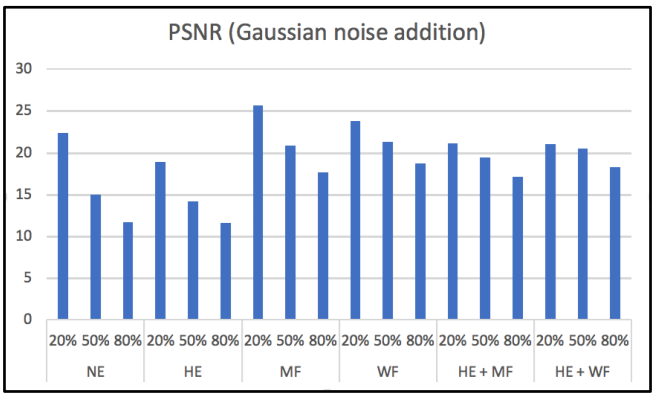

(b)

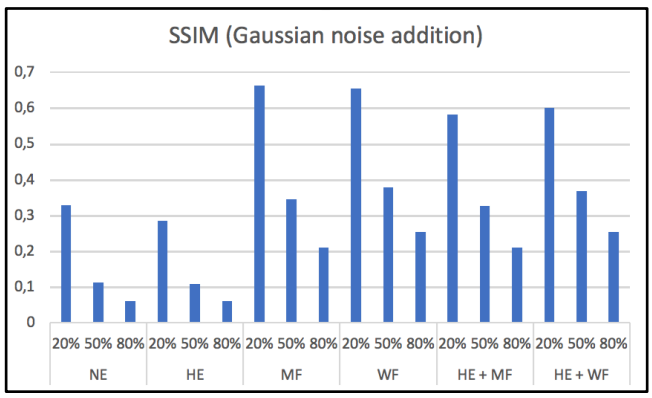

(c)

Figure 6. Three parameters to assess the image enhancement methods with the Gaussian noise addition: (a) MSE; (b) PSNR; (c) SSIM

Figure 8 depicts the MSE graph (e.g., representing the PSNR and SSIM graphs) for the Gaussian and salt-and-pepper noise additions. This graph shows that the implementation of HE and the following modifications (HE + MF and HE + WF) for noisy images did not enhance the image quality. Similar results can be observed in the MSE, PSNR, and SSIM graphs before the HE and hybrid processes (HE + MF and HE + WF).

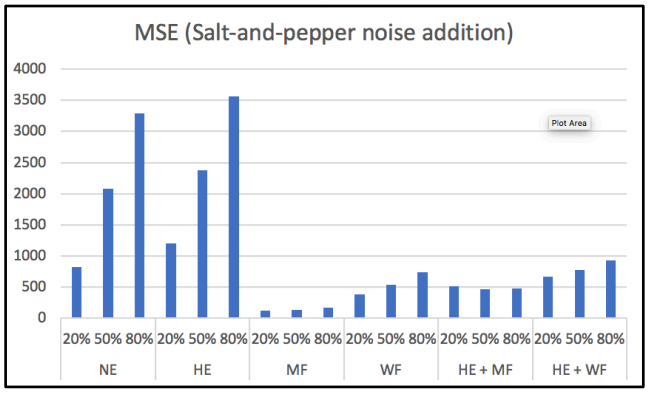

(a)

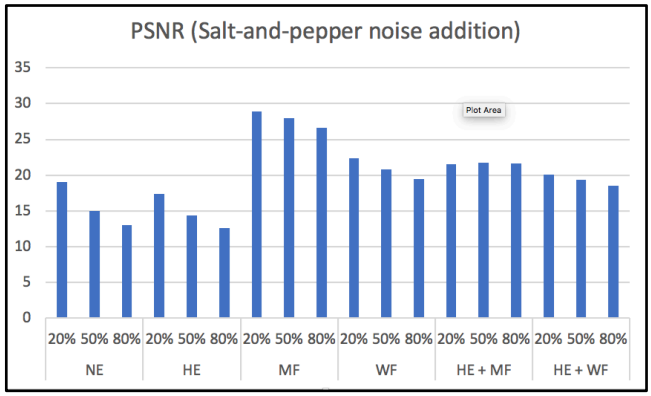

(b)

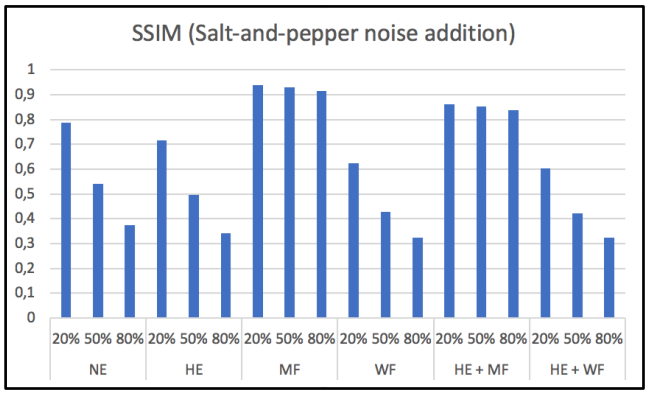

(c)

Figure 7. Three parameters to assess image enhancement methods with the salt-and-pepper noise addition: (a) MSE; (b) PSNR; (c) SSIM

HE and its hybrid methods were unable to remove noises. The average MSE in HE was the largest compared with the MSE in other methods. The overall average PSNR in HE was the lowest compared with the PSNR of other methods. This is because HE only equalizes the histogram but does not remove noises, so noises still persist after the process. This finding is consistent with that stated by Nithyananda *et al.* [14] and Zhao *et al.* [23].

V. Conclusions

The optimal methods that can be used for Gaussian and salt-and-pepper noisy images are WF and MF, respectively. HE and the two hybrid methods (HE + MF and HE + WF) do not generally enhance the image quality of Gaussian and salt-and-pepper noisy images. This is because HE only performs histogram arrangement but does not remove noises, so the

noise value remains, and this noise participates in the said process. The exception testing of hybrid method 2 (HE + WF) resulted in the maximum SSIM in high-Gaussian-noise images (80%). Meanwhile, MF resulted in the minimum MSE and maximum PSNR for low-Gaussian-noise images (20%).

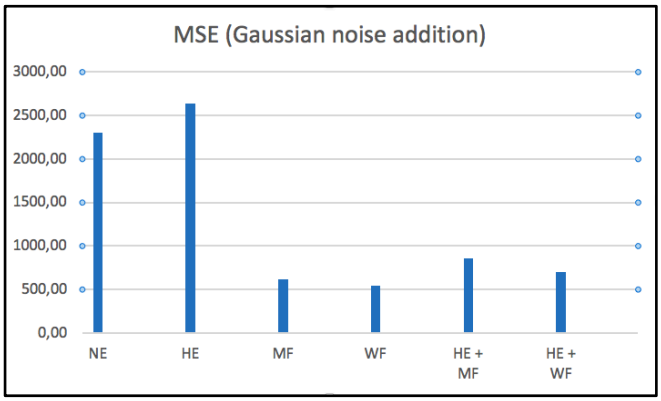

(a)

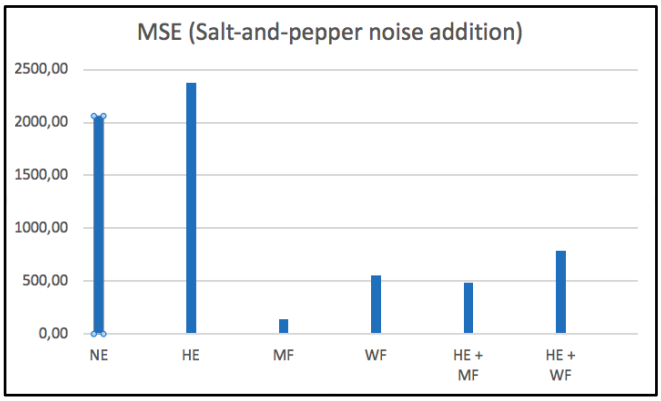

(b)

Figure 8. MSE to assess the image enhancement method on (a) Gaussian noise addition and (b) salt-and-pepper noise addition

REFERENCES

[1] P. Pangestu, D. Gunawan, and S. Hansun, "Histogram equalization implementation in the processing phase on optical character recognition," *2017 International Journal of Technology*, Vol. 8 no. 5, Universitas Multimedia Nusantara, 2017.

[2] Erwin, A. Nevriyanto dan D. Purnamasari., "Image enhancement using the image sharpening, contrast enhancement, and standard median filter (noise removal) with pixel-based and human visual system-based measurements," *2017 International Conference on Electrical Engineering and Computer Science* (ICECOS), 2017.

[3] G. George, R. M. Oommen, S. Shelly, S. S. Philipose and A. M. Varghese, "A survey on various median filtering techniques for removal of impulse noise from digital image," *2018 Conference on Emerging Devices and Smart Systems (ICEDSS)*, Tiruchengode, 2018, pp. 235-238.

[4] R. Kunsoth and M. Biswas, "Modified decision based median filter for impulse noise removal," *2016 International Conference on Wireless Communications, Signal Processing and Networking (WiSPNET)*, Chennai, 2016, pp. 1316-1319, doi: 10.1109/WiSPNET.2016.7566350.

[5] J. Jezebel Priestley, V. Nandhini and V. Elamaran, "A decision based switching median filter for restoration of images corrupted by high density impulse noise," *2015 International Conference on Robotics, Automation, Control and Embedded Systems (RACE)*, Chennai, 2015, pp. 1-5, doi: 10.1109/RACE.2015.7097287.

[6] M. S. Darus, S. N. Sulaiman, I. S. Isa, Z. Hussain, N. M. Tahir and N. A. M. Isa, "Modified hybrid median filter for removal of low density random-valued impulse noise in images," *2016 6th IEEE International Conference on Control System, Computing and Engineering (ICCSCE)*, Batu Ferringhi, 2016, pp. 528-533, doi: 10.1109/ICCSCE.2016.7893633.

[7] S. Khatri and H. Kasturiwale, "Quality assessment of Median filtering techniques for impulse noise removal from digital images," *2016 3rd International Conference on Advanced Computing and Communication Systems (ICACCS)*, Coimbatore, 2016, pp. 1-4, doi: 10.1109/ICACCS.2016.7586331.

[8] P. Goyal and V. Chaurasia, "Application of median filter in removal of random valued impulse noise from natural images," *2017 International conference of Electronics, Communication and Aerospace Technology (ICECA)*, Coimbatore, 2017, pp. 125-128, doi: 10.1109/ICECA.2017.8203657.

[9] S. Lahmiri and M. Boukadoum, "Hybrid Wiener and partial differential equations filter for biomedical image denoising," *2016 14th IEEE International New Circuits and Systems Conference (NEWCAS)*, Vancouver, BC, 2016, pp. 1-4, doi: 10.1109/NEWCAS.2016.7604754.

[10] F. Baselice, G. Ferraioli, V. Pascazio and G. Schirinzi, "Enhanced wiener filter for despeckling ultra-sound images," *2016 IEEE Nuclear Science Symposium, Medical Imaging Conference and Room-Temperature Semiconductor Detector Workshop (NSS/MIC/RTSD)*, Strasbourg, 2016, pp. 1-3, doi: 10.1109/NSSMIC.2016.8069428.

[11] N. Arazm, A. Sahab and M. F. Kazemi, "Noise reduction of SEM images using adaptive wiener filter," *2017 IEEE International Conference on Cybernetics and Computational Intelligence (CyberneticsCom)*, Phuket, 2017, pp. 50-55, doi: 10.1109/CYBERNETICSCOM.2017.8311683.

[12] A. H. Sheer and A. A. Al-Ani, "The effect of regularization parameter within non-blind restoration algorithm using modified iterative wiener filter for medical image," *2018 1st Annual International Conference on Information and Sciences (AiCIS)*, Fallujah, Iraq, 2018, pp. 77-81, doi: 10.1109/AiCIS.2018.00026.

[13] P. Kalavathi and T. Priya, "Removal of impulse noise using histogram-based localized wiener filter for MR brain image restoration," *2016 IEEE International Conference on Advances in Computer Applications (ICACA)*, Coimbatore, 2016, pp. 4-8, doi: 10.1109/ICACA.2016.7887913.

[14] C. R. Nithyananda, A. C. Ramachandra and Preethi, "Review on histogram equalization based image enhancement techniques," *2016 International Conference on Electrical, Electronics, and Optimization Techniques (ICEEOT)*, Chennai, 2016, pp. 2512-2517, doi: 10.1109/ICEEOT.2016.7755145.

[15] T. Celik and T. Tjahjadi, "Automatic image equalization and contrast enhancement using Gaussian mixture modeling," *IEEE Transactions on Image Processing*, 2012, 21(1): pp. 145-156.

[16] B.N. Mohapatra and P.P. Panda, "Histogram equalization and noise removal process for enhancement of image," *ACCENTS Transactions on Image Processing and Computer Vision,* Vol. 3(9), 2017, pp. 22-25, doi: 10.19101/TIPCV.2017.39015.

[17] S. Mehta, "Hybrid Wiener median Filter," *International Journal of Research and Analytical Reviews,* Vol. 4(4), 2017, pp. 238-241.

[18] The Mathworks, Inc., "Image processing toolbox™ User's Guide," 2019, Natick, MA.

[19] G. Gupta, "Algorithm for image processing using improved median filter and comparison of mean, median and improved median filter," *International Journal of Soft Computing and Engineering*, Vol 1(5), 2011, pp. 304-311.

[20] S. Kumar, M. Kumar, R. Rashid, and N. Agrawal, "A comparative analysis on image denoising using different median filter methods," *International Journal for Reasearch and Engineering Technology*, Vol. 5(8), 2017, pp. 231-239.

[21] S. Vishaga and S. L. Das, "A survey on switching median filters for impulse noise removal," *2015 International Conference on Circuits, Power and Computing Technologies [ICCPCT-2015]*, Nagercoil, 2015, pp. 1-6.

[22] B. Sravani and M. V. Nageswara Rao, "Removing of high density salt and pepper noise using fuzzy median filter," *2014 International Conference on High Performance Computing and Applications (ICHPCA)*, Bhubaneswar, 2014, pp. 1-6.

[23] Y. Zhao, N. D. Georganas and E. M. Petriu, "Applying contrast-limited adaptive histogram equalization and integral projection for facial feature enhancement and detection," *2010 IEEE Instrumentation & Measurement Technology Conference Proceedings*, Austin, TX, 2010, pp. 861-866, doi: 10.1109/IMTC.2010.5488048.